Supporting Information

Ultralight, compressible and multifunctional carbon aerogels based on natural tubular cellulose

Junping Zhang,[a]* Bucheng Li,[a] Lingxiao Li,[ab] and Aiqin Wang[a]

Experimental Section

Materials

Raw KFs were purchased from Shanghai Panda Co., Ltd., China. SC, anhydrous ethanol, acetic acid, methylene blue, oil red O, dichloroethane, cyclohexane, *n*-hexane, petroleum ether, acetone, tetrachloromethane and toluene were purchased from China National Medicines Co., Ltd., China. The Fe_3O_4 nanoparticles (99.5%, 8-16 nm in size) were purchased from Aladdin Industrial Corporation. Commercial petrol was purchased from Sinopec, Lanzhou, China. Other reagents used were all of analytical grade. Deionized water was used throughout the experiment. All chemicals were used as received without further purification.

Preparation of SC-KFs

50 g of the raw KFs were washed in turn with 1 L of water and 1 L of ethanol. SC (4.0 g) was dissolved in 400 mL of deionized water in a flask equipped with a mechanical stirrer and a thermometer. The pH of the SC solution was adjusted to 4.5 using 1.2 mL of acetic acid. Afterwards, 4.0 g of KFs was added and stirred at 1000 rpm and 80 ℃ for 2 h. Finally, SC-KFs were washed with deionized water until pH 6, and then washed with anhydrous ethanol for three times to remove the residual water.

Fabrication of UCM aerogel

The SC-KFs suspension in ethanol was homogenized at 12000 rpm for 20 min. After that, the suspension was poured into the desired mould, filtered to yield the SC-KFs aerogels with

diverse shapes, and then dried in an oven at 60 ℃ for 6 h. Finally, the SC-KFs aerogels was pyrolyzed in a tubular furnace at 1000 ℃ for 2 h in an N_2 atmosphere to form the UCM aerogels. In order to remove the air trapped in the sample, the furnace was repeatedly evacuated and charged with N_2 for six times. The furnace was heated up to 1000 ℃ at a heating rate of 5 ℃ min^{-1} and held at 1000 ℃ for 2 h, and then cooled down naturally to room temperature.

Measurement of liquid absorption capacity

A piece of sample was immersed in an organic liquid at room temperature. The sample was taken out of the liquid after 1 min, drained for several seconds and wiped with filter paper to remove excess liquid. The liquid absorption capacity *k* of the sample was determined by weighing the sample before and after oil absorption and calculated according to the following equation:

$$k = (m_t - m_i)/m_i$$

where m_t is the weight of the wet sample with liquid (g) and m_i is the weight of the dry sample (g). Measurements of the weight of the samples were completed in ten seconds after taken out of the oils to avoid the influence of liquid evaporation on accuracy of the results.

Fabrication of UCM/Fe_3O_4 aerogels

The UCM/Fe_3O_4 aerogels were prepared by a dip-coating method. The dip coating solution was prepared by adding the Fe_3O_4 nanoparticles into ethanol (1.25 mg mL^{-1}) followed by ultrasonication for 10 min. Then, a piece of the UCM aerogel was immersed in the as-prepared coating solution for 2 min. Finally, the coated sample was dried at 60 ℃ in an oven for 2 h.

Characterization

The micrographs of the samples were taken using a field emission scanning electron microscope (SEM, JSM- 6701F, JEOL). Before SEM observation, all samples were fixed on

aluminum stubs and coated with gold (~7 nm). Digital micrographs of samples were taken using a Leica DM1000 microsystem (CMC GmbH, Germany). XRD patterns were obtained on X'pert PRO diffractometer with working conditions of Cu Kα, 30 mA and 40 kV (λ = 1.54060 Å). The scanning was made at room temperature between 10 and 60 ° in 2θ with a scanning speed of 0.02 ° per second. FTIR spectra of the samples were recorded on a Nicolet NEXUS FTIR spectrometer using potassium bromide pellets. X-ray photoelectron spectra (XPS) were obtained using a VG ESCALAB 250 Xi spectrometer equipped with a monochromated Al Kα X-ray radiation source and a hemispherical electron analyzer. Spectra were recorded in the constant pass energy mode with a value of 100 eV, and all binding energies were calibrated using the C 1s peak at 284.6 eV as the reference. TGA analysis was carried out using a STA 6000 (PerkinElmer Instrument Co., Ltd. USA) to investigate thermal stability of the samples over a temperature range of 25 to 650 ℃ at a rate of 10 ℃/min under N_2 atmosphere. The mechanical properties of samples were measured using a universal testing machine (CMT4304, Shenzhen SANS Test Machine Co. Ltd., Shenzhen, China) equipped with a 200 N load cell at room temperature. The strain ramp rate was 25 mm min^{-1}. A vibrating-sample magnetometer (VSM) (Lake Shore, 735 VSM, Model 7304, USA) was used to test the magnetic properties of the samples. The electric resistance of the UCM aerogels was measured using a digital multimeter. Measurement of contact angle was performed at 25 ℃ using water drops of 7 μL on a Contact Angle System OCA 20 (Dataphysics, Germany). For the contact angle measurement, the syringe was positioned in a way that the droplet of water could contact surface of the samples before leaving the needle. All the measurements of compressive stress-strain curves, variation of R_t/R_0 with compressive strain, absorption capacity for organic liquids as well as contact angles of the sampels were carried out for six times and the average values were presented.

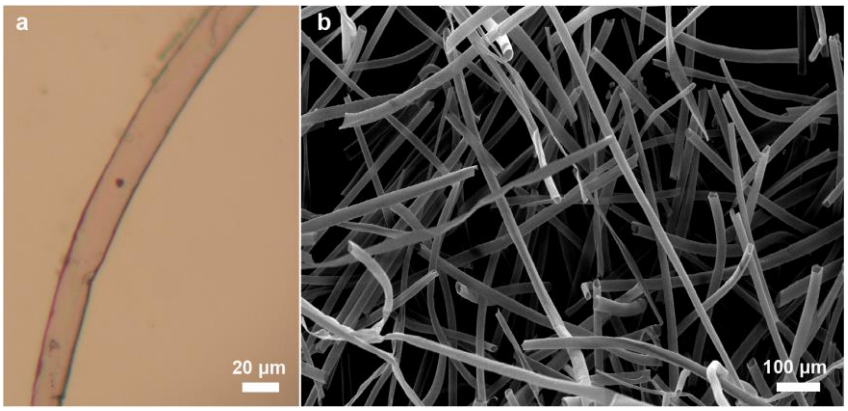

Fig. S1. (a) Micrograph of a single KF and (b) SEM image of the SC-KFs aerogel.

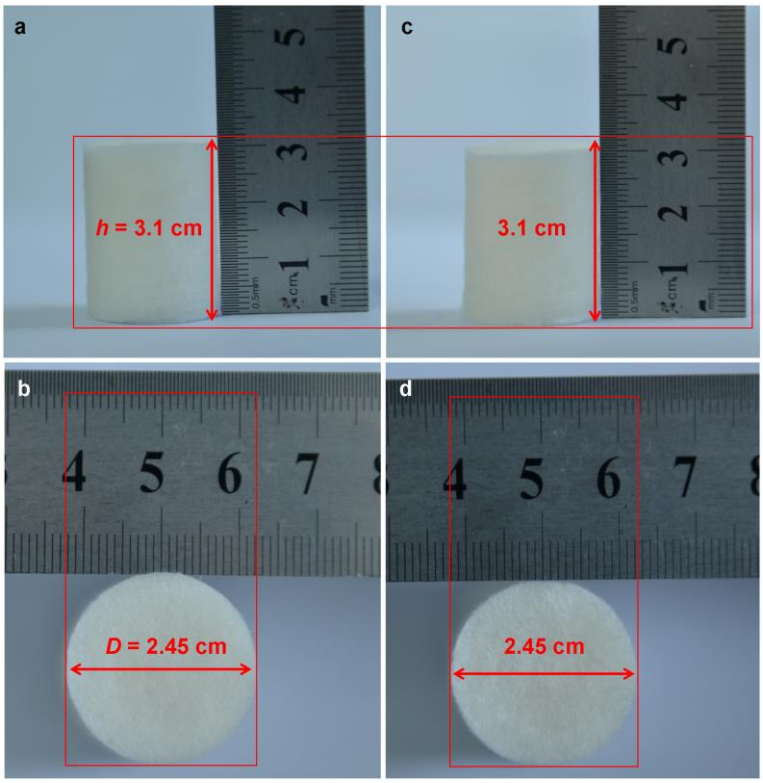

Fig. S2. Digital images of SC-KFs aerogels (a, b) before and (c, d) after oven drying at 60 ℃.

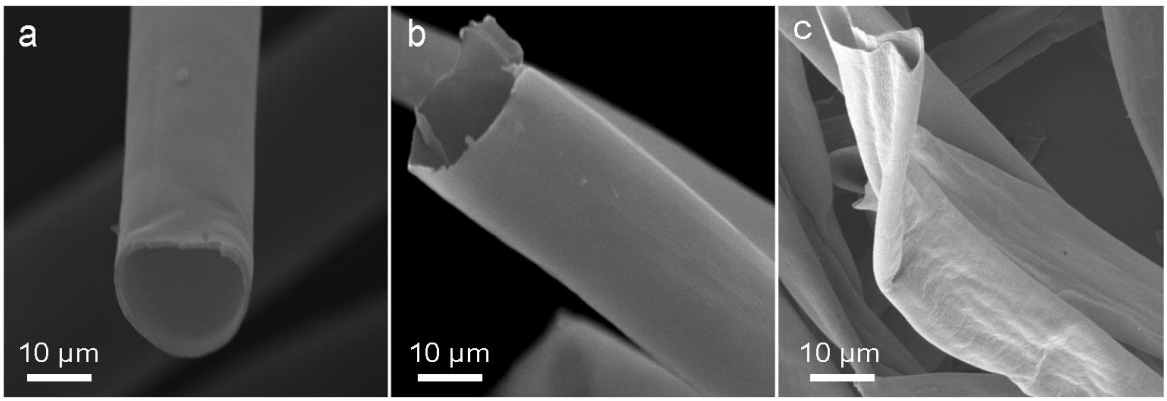

Fig. S3. SEM images of (a) KFs, (b) SC-KFs and (c) the UCM aerogel (1000 ℃, 2 h).

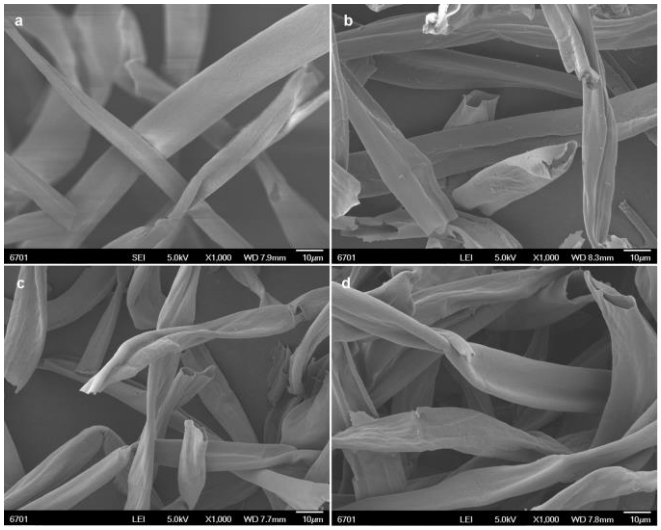

Fig. S4. SEM images of fibers of the UCM aerogels pyrolyzed at (a) 400 ℃, (b) 600 ℃, (c) 800 ℃ and (d) 1000 ℃ for 2 h.

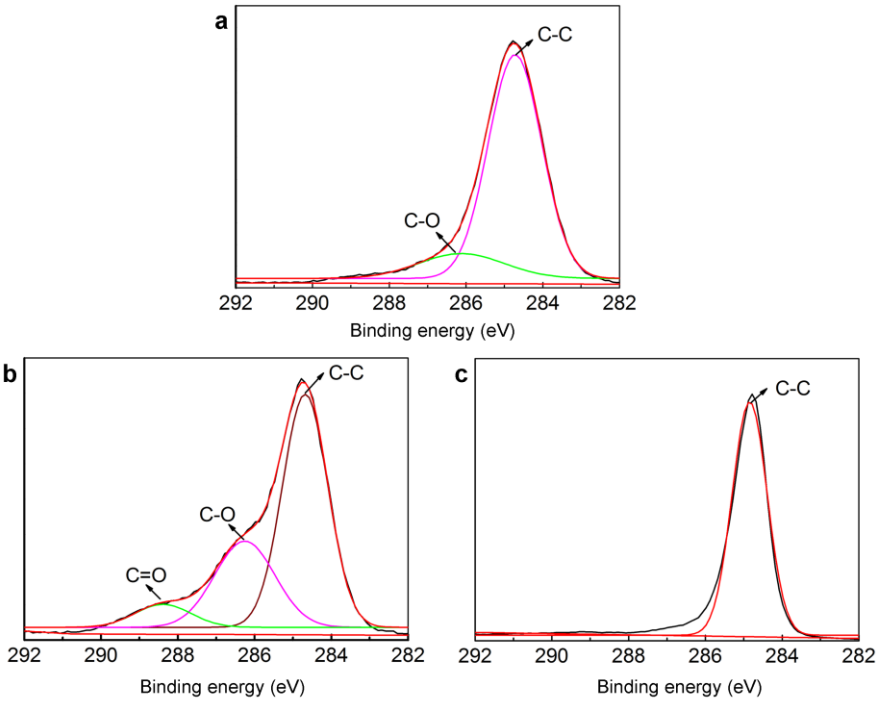

Fig. S5. High-resolution C 1s spectra of (a) KFs, (b) SC-KFs and (c) the UCM aerogel (1000 ℃).

In the C 1s spectrum of KFs, the two peaks at 284.4 eV (C-C and -C-H) and 286.1 eV (C-O) indicate that KFs mainly consist of cellulose and lignin.[1] In the C 1s spectrum of SC-KFs, the new peak at 288.4 eV (O-C-O and C=O) suggests that carbonyl species are formed by SC oxidation.

Table S1. Surface chemical composition of KFs, SC-KFs and the UCM aerogel.

Samples	KFs	SC-KFs	UCM aerogel
C (at.%)	89.29	76.38	96.39
O (at.%)	10.71	23.62	3.61

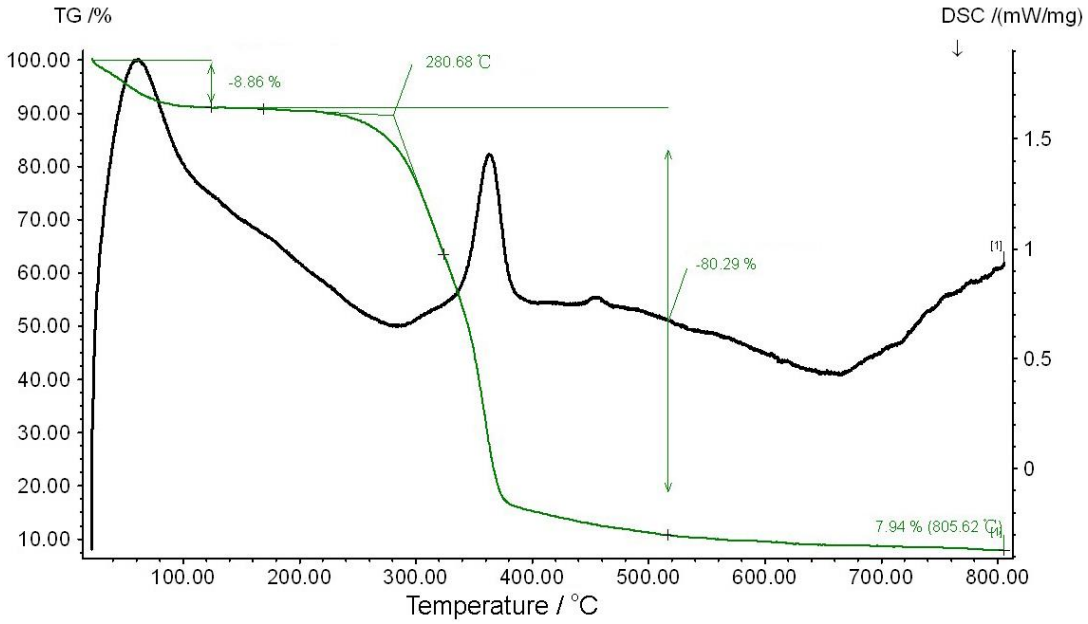

Fig. S6. TGA and DSC curves of SC-KFs obtained in an N_2 atmosphere.

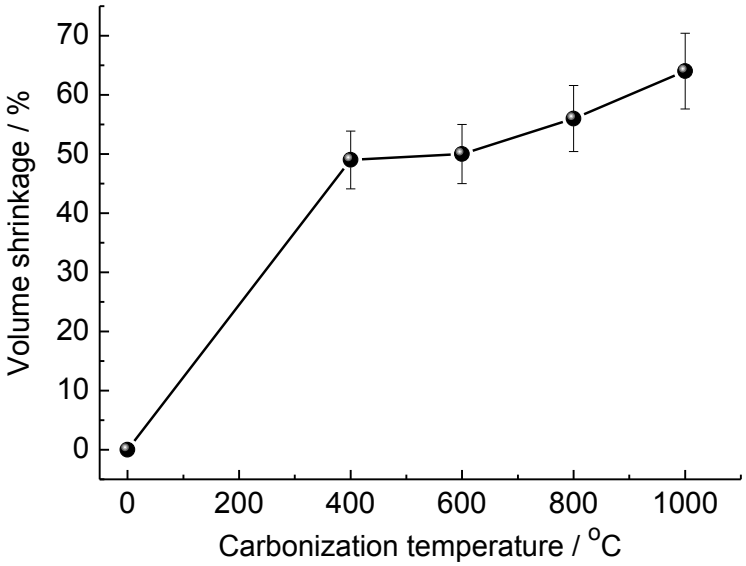

Fig. S7. Variation of volume shrinkage of the UCM aerogels with pyrolysis temperature.

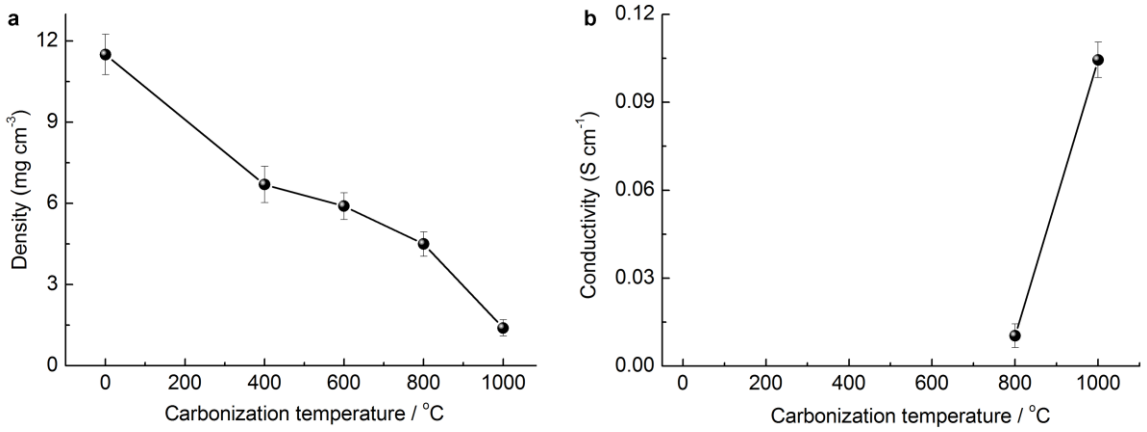

Fig. S8. (a) Density and (b) conductivity ofthe UCM aerogels pyrolyzed at different temperature for 2 h.

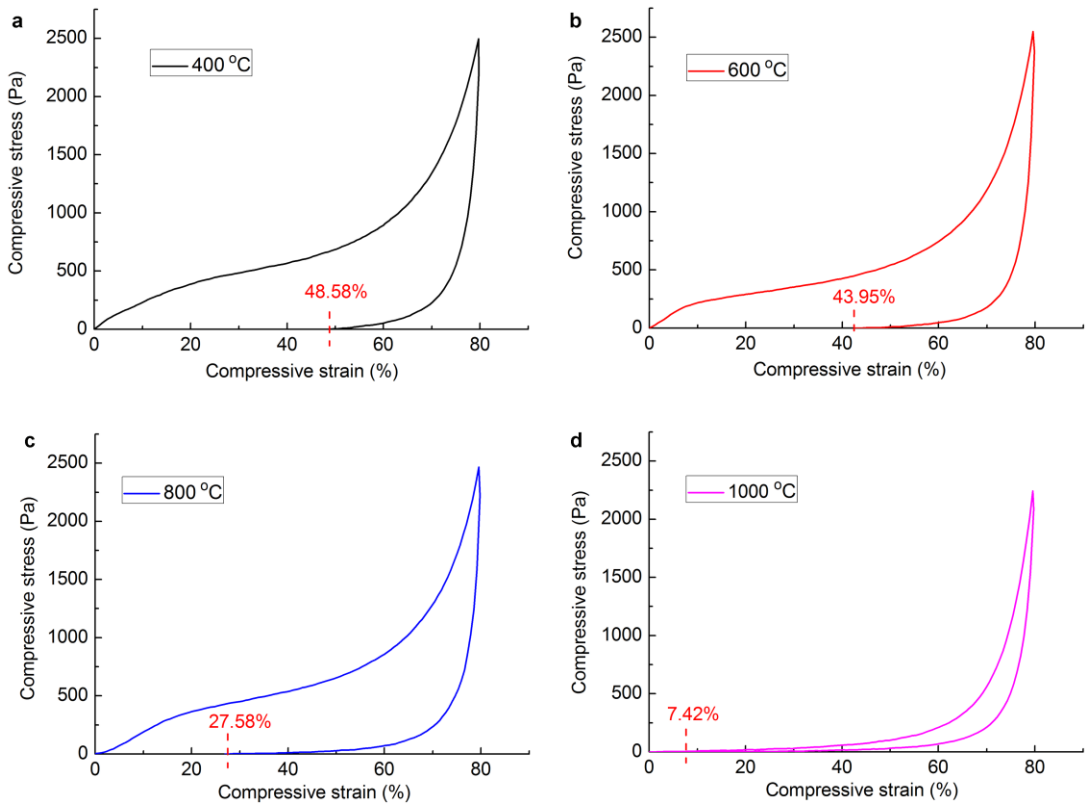

Fig. S9. (a) Compressive stress-strain curves ofthe UCM aerogels pyrolyzed at (a) 400 ℃, (b) 600 ℃, (c) 800 ℃ and (d) 1000 ℃ for 2 h.

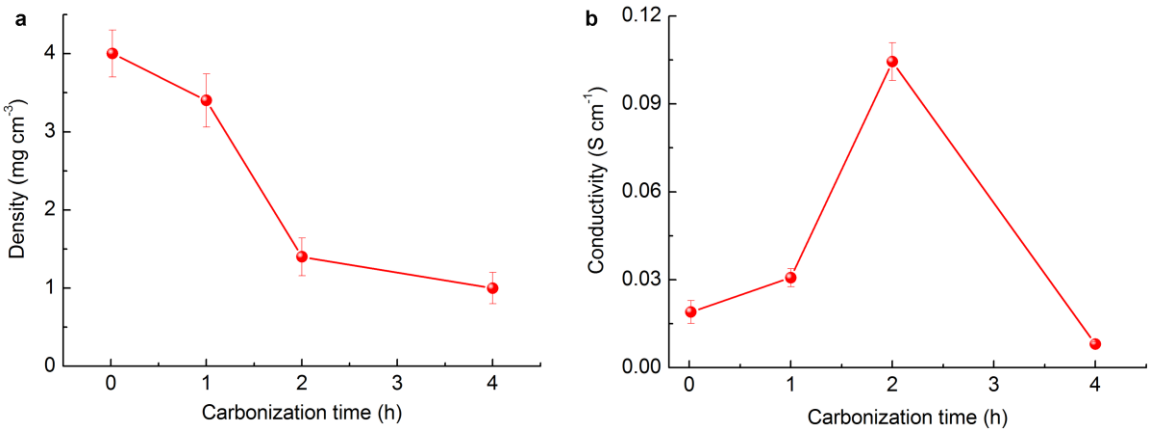

Fig. S10. (a) Density and (b) conductivity ofthe UCM aerogels pyrolyzed at 1000 ℃ for different time.

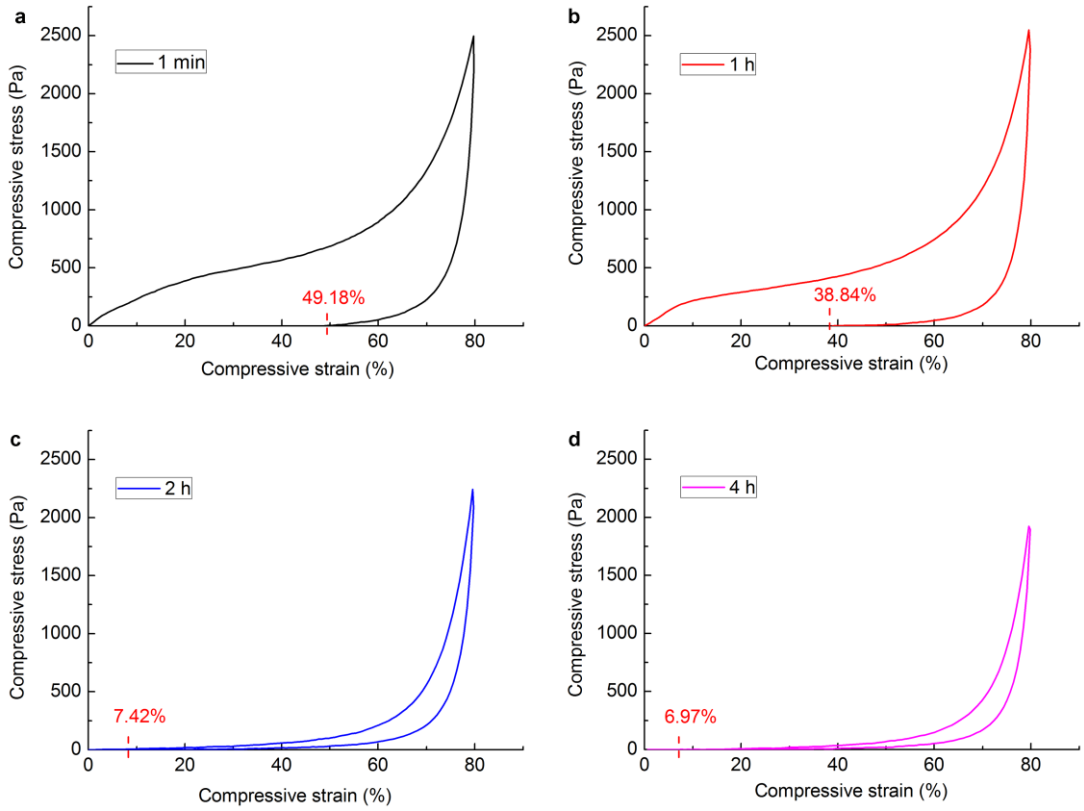

Fig. S11. (a) Compressive stress-strain curves ofthe UCM aerogels pyrolyzed at 1000 ℃ for (a) 1 min, (b) 1 h, (c) 2 h and (d) 4 h.

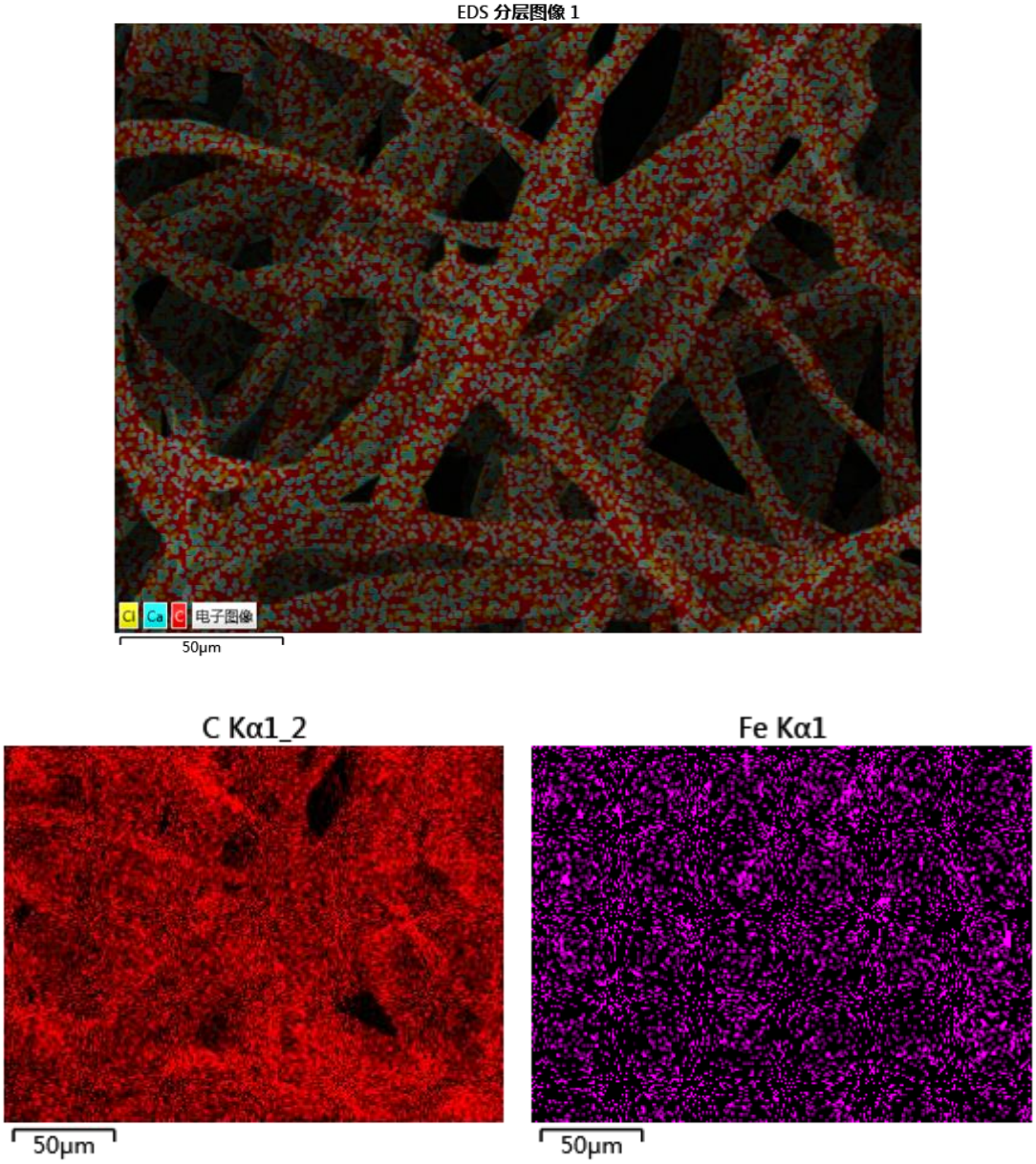

Fig. S12. SEM image of the UCM/Fe_3O_4 aerogel and EDS elemental maps of C and Fe in the UCM/Fe_3O_4 aerogel.

Table S2. Building blocks, methods, density, conductivity and compressibility of the previously reported aerogels and the UCM aerogel in this study.

Samples	**Building blocks**	**Methods**	**Density (mg cm^{-3})**	**Conductivity (S cm^{-1})**	**Compressibility**	**Ref.**
Silicone aerogel	Silanes	Supercritical drying	150	-	85% strain	[2]
Silicone aerogel	Silanes	Vacuum-drying	64	-	60% strain	[3]
Silicone aerogel	Silanes	Oven-drying	120	-	70% strain	[4]
Cellulose aerogel	Bacterial cellulose &$FeSO_4$/$CoCl_2$	Freeze-drying	-	-	-	[5]
Nanocellulose aerogel	Nanocellulose	Freeze-drying	30	-	-	[6]
CNTs aerogel	CNTs	Freeze-drying	4	0.67	95% strain	[7]
CNTs sponge	Ferrocene	CVD	5~10	1.67	80% strain	[8]
Graphene foam	CH_4 & Ni foam	Templating and CVD	5	10	-	[9]
Graphene foam	CH_4 & SiO_2 aerogel	Templating and CVD	1.8~100	0.1~100	95% strain	[10]
Graphene foam	Graphene oxide	Freeze-drying and pyrolysis	2.1	12	-	[11]
Graphene aerogel	Graphene oxide	Freeze-drying and pyrolysis	56	49	-	[12]
Graphene aerogel	CNTs	Supercritical drying	9.33	0.36	80% strain	[13]
Graphene aerogel	Graphene oxide	Freeze-drying	3~5	-	90% strain	[14]
Graphene aerogel	Graphene oxide	3D printing and Supercritical drying	31~123	0.87~2.78	50% strain	[15]

Nanocellulose/graphene foam	Nanocellulose, graphene oxide &sepiolite	Freeze-drying	0.12	-	90% strain	[16]
Nanocellulose/CNTs aerogel	Nanocellulose & CNTs	Freeze-drying	20	1.8	95% strain	[17]
Nanocellulose/CNTs aerogel	Nanocellulose & CNTs	LbL assembly and freeze-drying	-	1.2×10^{-3}	80% strain	[18]
CNTs/graphene aerogel	CNTs & graphene oxide	Freeze-drying	0.75	0.006	50% strain	[19]
Carbon sponge	Silver &PVA	Freeze-drying and pyrolysis	3.8	128	95% strain	[20]
Carbon/silica aerogel	Polyacrylonitrile& silica	Freeze-drying and pyrolysis	0.12	0.25	80% strain	[21]
Carbon foam	Polyacrylic acid	Templating	3.9	-	-	[22]
Carbon aerogel	Glucose	Templating and freeze-drying	3.3	-	80% strain	[23]
Carbon aerogel	Raw cotton	Pyrolysis	12	-	-	[24]
Carbon aerogel	Bacterial cellulose	Freeze-drying and pyrolysis	4~6	-	90% strain	[25]
Carbon aerogel	Waste paper	Freeze-drying and pyrolysis	5.8	-	-	[26]
UCM aerogel	**Kapok fibers**	**Pyrolysis**	**1~2**	**0.10**	**80% strain**	**This work**

"-" means not avaliable.

Table S3. Comparison of absorption capacity of various absorbents and the UCM aerogel for oils and organic liquids.

Absorbents	**Absorption capacity (g g^{-1})**	**Cost**	**Ref.**
Superhydrophobic PU sponge	13~45	medium	[27]
Superhydrophobic PU sponge	20-45	low	[28]
Superhydrophobic PU sponge	18~26	medium	[29]
Superhydrophobic PU sponge	27-86	low	[30]
Superhydrophobic PU sponge	5-23	medium	[31]
Superhydrophobic PET sponge	3~5	low	[32]
Superhydrophobic sponge	54~165	medium	[33]
Superhydrophobic melamine sponge	79~195	low	[34]
Superhydrophobic nanowire membrane	5~20	medium	[35]
Superhydrophobic silicone sponge	6~18	medium	[4]
Superhydrophobic silicone sponge	6~14	medium	[36]
Silylated nanocellulose sponge	50~102	medium	[37]
Graphene sponge	20~86	high	[38]
CNTs sponge	88~170	high	[8]
CNTs/graphene aerogel	215~743	high	[19]
Carbon aerogel	56~188	low	[26]
Carbon/silica sponge	65~140	medium	[39]
Carbon aerogel	106~312	medium	[25]
Carbon aerogel	50~192	low	[24]
Carbon foam	40~115	high	[23]
Carbon foam	60~100	medium	[22]
UCM aerogel	**147~292**	**low**	**This work**

Movie S1. Strain-dependent brightness of the diode linked to a circuit using the UCM aerogel. This video highlights the strain-dependent electrical conductivity of UCM aerogels.

Movie S2. Oil absorption and oil/water separation using the UCM aerogel. This video highlights the high oil absorbency and separation efficiency of the UCM aerogel.

Movie S3. Burning the UCM aerogel with the flame of a spirit lamp (~500 ℃). This video highlights the excellent fire resistance of the UCM aerogel.

References

1. J. P. Zhang, L. Wu, Y. J. Zhang and A. Q. Wang, *J. Mater. Chem. A*, 2015, **3**, 18475-18482.
2. K. Kanamori, M. Aizawa, K. Nakanishi and T. Hanada, *Adv. Mater.*, 2007, **19**, 1589-1593.
3. Z. Wang, Z. Dai, J. Wu, N. Zhao and J. Xu, *Adv. Mater.*, 2013, **25**, 4494-4497.
4. L. Li, B. Li, L. Wu, X. Zhao and J. Zhang, *Chem. Commun.*, 2014, **50**, 7831-7833.
5. R. T. Olsson, M. A. S. Azizi Samir, G. Salazar Alvarez, BelovaL, StromV, L. A. Berglund, IkkalaO, NoguesJ and U. W. Gedde, *Nat. Nano.*, 2010, **5**, 584-588.
6. M. Kettunen, R. J. Silvennoinen, N. Houbenov, A. Nykänen, J. Ruokolainen, J. Sainio, V. Pore, M. Kemell, M. Ankerfors and T. Lindström, *Adv. Funct. Mater.*, 2011, **21**, 510-517.
7. J. Zou, J. Liu, A. S. Karakoti, A. Kumar, D. Joung, Q. Li, S. I. Khondaker, S. Seal and L. Zhai, *ACS Nano*, 2010, **4**, 7293-7302.
8. X. Gui, J. Wei, K. Wang, A. Cao, H. Zhu, Y. Jia, Q. Shu and D. Wu, *Adv. Mater.*, 2010, **22**, 617-621.
9. Z. Chen, W. Ren, L. Gao, B. Liu, S. Pei and H.-M. Cheng, *Nat. Mater.*, 2011, **10**, 424-428.
10. H. Bi, I. W. Chen, T. Lin and F. Huang, *Adv. Mater.*, 2015, **27**, 5943-5949.
11. Y. Zhao, C. Hu, Y. Hu, H. Cheng, G. Shi and L. Qu, *Angew. Chem. Int. Ed.*, 2012, **124**,

11533-11537.

12. Z. Xu, Y. Zhang, P. Li and C. Gao, *ACS Nano*, 2012, **6**, 7103-7113.
13. Q. Peng, Y. Li, X. He, X. Gui, Y. Shang, C. Wang, C. Wang, W. Zhao, S. Du, E. Shi, P. Li, D. Wu and A. Cao, *Adv. Mater.*, 2014, **26**, 3241-3247.
14. H. Hu, Z. Zhao, W. Wan, Y. Gogotsi and J. Qiu, *Adv. Mater.*, 2013, **25**, 2219-2223.
15. C. Zhu, T. Y. Han, E. B. Duoss, A. M. Golobic, J. D. Kuntz, C. M. Spadaccini and M. A. Worsley, *Nat. Commun.*, 2015, **6**, 6962.
16. B. Wicklein, A. Kocjan, G. Salazar-Alvarez, F. Carosio, G. Camino, M. Antonietti and L. Bergström, *Nat. Nano.*, 2015, **10**, 277-283.
17. M. Wang, I. V. Anoshkin, A. G. Nasibulin, J. T. Korhonen, J. Seitsonen, J. Pere, E. I. Kauppinen, R. H. A. Ras and O. Ikkala, *Adv. Mater.*, 2013, **25**, 2428-2432.
18. M. Hamedi, E. Karabulut, A. Marais, A. Herland, G. Nyström and L. Wågberg, *Angew. Chem. Int. Ed.*, 2013, **52**, 12038-12042.
19. H. Sun, Z. Xu and C. Gao, *Adv. Mater.*, 2013, **25**, 2554-2560.
20. H.-B. Yao, G. Huang, C.-H. Cui, X.-H. Wang and S.-H. Yu, *Adv. Mater.*, 2011, **23**, 3643-3647.
21. Y. Si, J. Yu, X. Tang, J. Ge and B. Ding, *Nat. Commun.*, 2014, **5**, 5802.
22. N. Chen and Q. Pan, *ACS Nano*, 2013, **7**, 6875-6883.
23. H.-W. Liang, Q.-F. Guan, L.-F. Chen, Z. Zhu, W.-J. Zhang and S.-H. Yu, *Angew. Chem. Inter. Ed.*, 2012, **51**, 5101-5105.
24. H. Bi, Z. Yin, X. Cao, X. Xie, C. Tan, X. Huang, B. Chen, F. Chen, Q. Yang, X. Bu, X. Lu, L. Sun and H. Zhang, *Adv. Mater.*, 2013, **25**, 5916-5921.
25. Z. Y. Wu, C. Li, H. W. Liang, J. F. Chen and S. H. Yu, *Angew. Chem. Int. Ed.*, 2013, **52**, 2925-2929.
26. H. Bi, X. Huang, X. Wu, X. Cao, C. Tan, Z. Yin, X. Lu, L. Sun and H. Zhang, *Small*, 2014, **10**, 3544-3550.

27. L. Wu, L. Li, B. Li, J. Zhang and A. Wang, *ACS Appl. Mater. Interfaces*, 2015, **7**, 4936-4946.

28. B. C. Li, L. X. Li, L. Wu, J. P. Zhang and A. Q. Wang, *ChemPlusChem*, 2014, **79**, 850-856.

29. Q. Zhu and Q. Pan, *ACS Nano*, 2014, **8**, 1402-1409.

30. H. Sun, A. Li, Z. Zhu, W. Liang, X. Zhao, P. La and W. Deng, *ChemSusChem*, 2013, **6**, 1057-1062.

31. A. Li, H. X. Sun, D. Z. Tan, W. J. Fan, S. H. Wen, X. J. Qing, G. X. Li, S. Y. Li and W. Q. Deng, *Energy Environ. Sci.*, 2011, **4**, 2062-2065.

32. L. Wu, J. P. Zhang, B. C. Li and A. Q. Wang, *Polym. Chem.*, 2014, **5**, 2382-2390.

33. D. D. Nguyen, N.-H. Tai, S.-B. Lee and W.-S. Kuo, *Energy Environ. Sci.*, 2012, **5**, 7908-7912.

34. C. Ruan, K. Ai, X. Li and L. Lu, *Angew. Chem. Int. Ed.*, 2014, **53**, 5556-5560.

35. J. Yuan, X. Liu, O. Akbulut, J. Hu, S. L. Suib, J. Kong and F. Stellacci, *Nat. Nanotechnol.*, 2008, **3**, 332-336.

36. G. Hayase, K. Kanamori, M. Fukuchi, H. Kaji and K. Nakanishi, *Angew. Chem. Int. Ed.*, 2013, **52**, 1986-1989.

37. Z. Zhang, G. Sèbe, D. Rentsch, T. Zimmermann and P. Tingaut, *Chem. Mater.*, 2014, **26**, 2659-2668.

38. H. Bi, X. Xie, K. Yin, Y. Zhou, S. Wan, L. He, F. Xu, F. Banhart, L. Sun and R. S. Ruoff, *Adv. Funct. Mater.*, 2012, **22**, 4421-4425.

39. M. H. Tai, B. Y. Tan, J. Juay, D. D. Sun and J. O. Leckie, *Chem. Eur. J.*, 2015, **21**, 5395-5402.